Check for updates

Electrical properties of copper- and silver-containing superionic $(Cu_{1-x}Ag_x)_7SiS_5I$ mixed crystals with argyrodite structure

I.P. Studenyak[a,*], A.I. Pogodin[a], V.I. Studenyak[a], V.Yu. Izai[a], M.J. Filep[a], O.P. Kokhan[a], M. Kranjčec[b], P. Kúš[c]

[a] *Uzhhorod National University, Pidgirna St. 46, Uzhhorod 88000, Ukraine*
[b] *University North, J. Križanića St. 33, Varaždin 42000, Croatia*
[c] *Comenius University, Mlynska dolina, Bratislava 84248, Slovakia*

ABSTRACT

The copper and silver containing $(Cu_{1-x}Ag_x)_7SiS_5I$ mixed crystals with argyrodite structure have been grown by direct solidification using the Bridgman-Stockbarger technique. Measurements of electrical conductivity of mixed crystals by means of impedance spectroscopy were carried out in the frequency range from 2×10^1 Hz to 2×10^6 Hz and temperature range 292–378 K. Frequency dependences of total electrical conductivity were studied, Nyquist plots were constructed and analysed. The influence of $Cu^+ \rightarrow Ag^+$ cation substitution on the total electrical conductivity, on the electronic and ionic components of the electrical conductivity as well as on their activation energies for $(Cu_{1-x}Ag_x)_7SiS_5I$ mixed crystals was investigated.

1. Introduction

Cu_7SiS_5I and Ag_7SiS_5I crystals belong to the compounds with argyrodite structure [1,2]. They are characterized by high values of electrical conductivity and small values of activation energy [3,4]. This raises a practical interest in these materials, associated with the possibility of their use for the needs of solid-state ionics, for example, in the role of accumulators, supercapacitors and electrochemical sensors [5–8]. The argyrodites one can obtained not only in crystalline forms, but in forms of composites, ceramics and thin films [6–9]. In the last year, for the preparation of new all-solid-state batteries the Li-containing argyrodites are actively studied [10–13].

The results of the structural and optical studies of mixed crystals based on Cu_7SiS_5I are given in Refs. [14, 15]. In Ref. [10], it was shown that Urbach behavior of the absorption edge is observed in $Cu_7(Ge_{1-x}Si_x)S_5I$ mixed crystals. At cationic $Ge^{+4} \rightarrow Si^{+4}$ substitution a nonlinear increase of the optical pseudogap as well as the typical for mixed crystals variation of Urbach energy are revealed [15].

The purpose of this work was to synthesize and growth of $(Cu_1Ag_x)_7SiS_5I$ mixed crystals, study the frequency and temperature dependences of electrical conductivity, as well as the study of the compositional behavior of the total electrical conductivity, the ionic and electronic conductivity components and the activation energy of mixed crystals under investigations.

2. Experimental

Synthesis of Cu_7SiS_5I and Ag_7SiS_5I compounds was carried out from the simple substances: copper (99.999%), silver (99.995%), silicon (99.99997%), sulfur (99.999%), and pre-synthesized binary cuprum (I) iodide and argentum (I) iodide, further purified by vacuum distillation and directional crystallization, respectively, taken in stoichiometric ratios in vacuated to 0.13 Pa quartz ampoules. The synthesis regime of Cu_7SiS_5I and Ag_7SiS_5I included step heating up to 723 K at a rate of 100 K/h (ageing during 48 h), further increase of temperature to 1470 K for Cu_7SiS_5I and 1230 K for Ag_7SiS_5I at a rate of 50 K/h and ageing at this temperature for 24 h. Alloys of Cu_7SiS_5I-Ag_7SiS_5I system were synthesized by a direct one-temperature method from the pre-synthesized Cu_7SiS_5I and Ag_7SiS_5I compounds. The synthesis mode included step heating at a rate of 100 K/h to 1023 K and ageing at that temperature for 24 h, further raising the temperature to 1470 K at a rate of 50 K/h and ageing at that temperature for 72 h. The annealing were performed at the temperature of 873 K during 120 h. Cooling to room temperature was carried out in the mode of the switched off oven.

Growth of $(Cu_1Ag_x)_7SiS_5I$ mixed crystals with (x = 0, 0.25, 0.5, 0.75, 1) by means of crystallization from the melt (Cu_7SiS_5I and Ag_7SiS_5I) and the melt solution ($(Cu_{1-x}Ag_x)_7SiS_5I$) was carried out in two-zone tubular resistance furnace (temperature of the melt zone constituted 1470 K (Cu_7SiS_5I), 1230 K (Ag_7SiS_5I), that of annealing

---

Table 1
Technological conditions of $(Cu_{1-x}Ag_x)_7SiS_5I$ mixed crystals growth.

Composition	Temperature of the melt zone (K)	Temperature of annealing zone (K)	Time of growth (hours)
Cu_7SiS_5I	1470	1023	168
$(Cu_{0.75}Ag_{0.25})_7SiS_5I$	1390	930	168
$(Cu_{0.5}Ag_{0.5})_7SiS_5I$	1280	850	168
$(Cu_{0.25}Ag_{0.75})_7SiS_5I$	1220	780	168
Ag_7SiS_5I	1230	800	168

zone - 1023 K and 800 K, respectively) using a quartz container of a special configuration. Technological conditions for growing mixed crystals are given in Table 1. In order to homogenize the melt, 24 h of ampoule ageing was performed at temperatures in the range 1470–1230 K (Table 1) in the melt zone. The crystal growth consists of the formation of the seed in the lower conical part of the container by the method of recrystallization during 24 h and the crystal build-up on the formed seed. The optimum rate of movement of the crystallization front constituted 0.4–0.5 mm/h, the annealing temperature was 1023–800 K (during 72 h), the cooling rate to room temperature was 5 K/h. By this method, $(Cu_1Ag_x)_7SiS_5I$ mixed crystals of dark gray color with a metallic luster (30–40 mm in length and 10–15 mm in diameter) were obtained.

The diffractograms of Cu_7SiS_5I and Ag_7SiS_5I compounds were indexed in a face-centred cubic cell $F\bar{4}3m$. The number and nature of the reflexes on the diffractograms for compounds of Cu_7SiS_5I-Ag_7SiS_5I system indicate that a continuous series of solid solutions is formed in the above mentioned system.

Investigation of the electrical conductivity of $(Cu_{1-x}Ag_x)_7SiS_5I$ (x = 0, 0.25, 0.5, 0.75, 1) mixed crystals was carried out by the method of impedance spectroscopy [16,17], in the frequency range from 2×10^1 Hz to 2×10^6 Hz and temperature range of 292–378 K using the high-precision LCR meter Keysight E4980A. The amplitude of the alternating current constituted 10 mV. The analysis of the measured dependences was carried out in Scribner ZView software.

Measurements were performed by a two-electrode method, on blocking gold contacts. Gold contacts for measurements were applied by chemical precipitation from solutions. As starting solutions, 0.02 M tetrachloro-aurat (III) sodium $Na[AuCl_4]$ and formalin solution $(40\%CH_2O + 8\%CH_3OH + 52\%H_2O)$ (deoxidant) were used in the ratio of 5/1 (selected experimentally). Precipitation was carried out at a temperature of not > 293 K. Increasing the temperature negatively affects the quality of the deposited film due to the growth of recovery rate.

3. Results and discussion

Fig. 1 presents the frequency dependences of total electrical conductivity for $(Cu_{1-x}Ag_x)_7SiS_5I$ mixed crystals. It is shown that for all crystals under investigation the total electrical conductivity is increased with the frequency increased (Fig. 1). However, for Cu_7SiS_5I (Fig. 1, curve 1) crystal, at the frequences range of 10^5 Hz - 10^6 Hz there is a insignificant decrease in the total electrical conductivity due to the effect of parasitic inductance caused by the high electrical conductivity values [17]. For detailed studies of frequency dependences of electrical conductivity and its separation into ionic and electronic components, a standard approach with the use of electrode equivalent circuits (EEC) [18] as well as their analysis on Nyquist plots were used. In the analysis of all samples the parasitic inductance of the cell ($\sim 4 \times 10^{-7}$H) is taken into account.

In the analysis of the plots, in which for Cu_7SiS_5I one semicircle is observed (Fig. 2a), the EEC is chosen, characterized by the presence of the electronic resistance R_e, parallelly to which the capacity of the double diffusion layer C_d is included, and the ion resistance of the
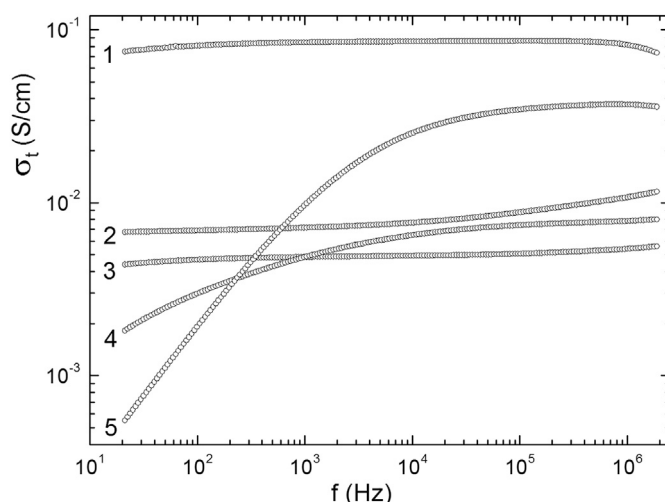

Fig. 1. The frequency dependences of the total electrical conductivity at T = 298 K for $(Cu_{1-x}Ag_x)_7SiS_5I$ mixed crystals: Cu_7SiS_5I (1), $(Cu_{0.75}Ag_{0.25})_7SiS_5I$ (2), $(Cu_{0.5}Ag_{0.5})_7SiS_5I$ (3), $(Cu_{0.25}Ag_{0.75})_7SiS_5I$ (4), Ag_7SiS_5I (5).

sample R_{ion}. Since Cu_7SiS_5I displayed that $\sigma_{ion} < \sigma_{el}$, but the value of ionic conductivity is high enough, there is a possibility of diffusion processes, which take place on the boundary of double diffusion layer. In this case, we introduced the Warburg element W_d (Fig. 2a) into the EEC, which allowed us to well describe the experimental results.

It should be noted that $(Cu_{1-x}Ag_x)_7SiS_5I$ mixed crystals with x = 0.25, 0.5, 0.75 are characterized by a more complex and disordered structure, which has affected the Nyquist plots. It is manifested in the changes in the quantity, shape and ratio of the semicircles sizes (Fig. 2). This, first of all, is associated with a change in the ratio of ionic to electronic conductivity during $Cu^+ \leftrightarrow Ag^+$ cationic substitution, which is caused by the structural changes in the process of mixed crystals formation. In turn, in the process of $Cu^+ \rightarrow Ag^+$ cationic substitution at transition from Cu_7SiS_5I to Ag_7SiS_5I the complications of the EEC selected to describe the experimental results are observed (Fig. 2). Thus, in the Nyquist plot for $(Cu_{0.75}Ag_{0.25})_7SiS_5I$ mixed crystal three semicircles are observed (Fig. 2b), whereas for each of $(Cu_{0.5}Ag_{0.5})_7SiS_5I$ (Fig. 2c) and $(Cu_{0.25}Ag_{0.75})_7SiS_5I$ (Fig. 2d) mixed crystals two semicircles are observed, respectively.

The low-frequency semicircles in Nyquist plots correspond to the diffusion relaxation processes at the electrode/crystal boundary and the electronic component of conductivity, which is determined by the included capacity of the double diffusion layer C_d parallel to the electronic resistance R_e for $(Cu_{0.75}Ag_{0.25})_7SiS_5I$ (Fig. 2b). For $(Cu_{0.5}Ag_{0.5})_7SiS_5I$ and $(Cu_{0.25}Ag_{0.75})_7SiS_5I$ mixed crystals (Fig. 2c and d), the contribution to the low-frequency semicircle is also introduced by the processes at the domain boundaries, which is expressed by the sequential incorporation of the resistance R_{db} and capacitance C_{db} of domain boundaries into EEC. As the content of silver increases during the transition from Cu_7SiS_5I to Ag_7SiS_5I, there is a shift of the low-frequency semicircle into the low-frequency area, which may be caused by the increasing influence of diffusion ionic processes, and due to the decrease in electron conductivity, also with the growth of ionic relaxation time as well. The semicircle in the middle-frequency area, which is observed only for $(Cu_{0.75}Ag_{0.25})_7SiS_5I$ mixed crystal (Fig. 2b) corresponds to the processes of ion transport at the domains boundaries R_{db}, which are characterized by the capacity C_{db}.

The high-frequency semicircles, in turn, are characterized by the processes of bulk ionic conductivity, which determines by the ion resistance R_{ion} for $(Cu_{0.75}Ag_{0.25})_7SiS_5I$ mixed crystal on the EEC, and in the case of $(Cu_{0.5}Ag_{0.5})_7SiS_5I$ and $(Cu_{0.25}Ag_{0.75})_7SiS_5I$ mixed crystals parallelly to the ion resistance, C_{ion} capacitance is included. Parallelly
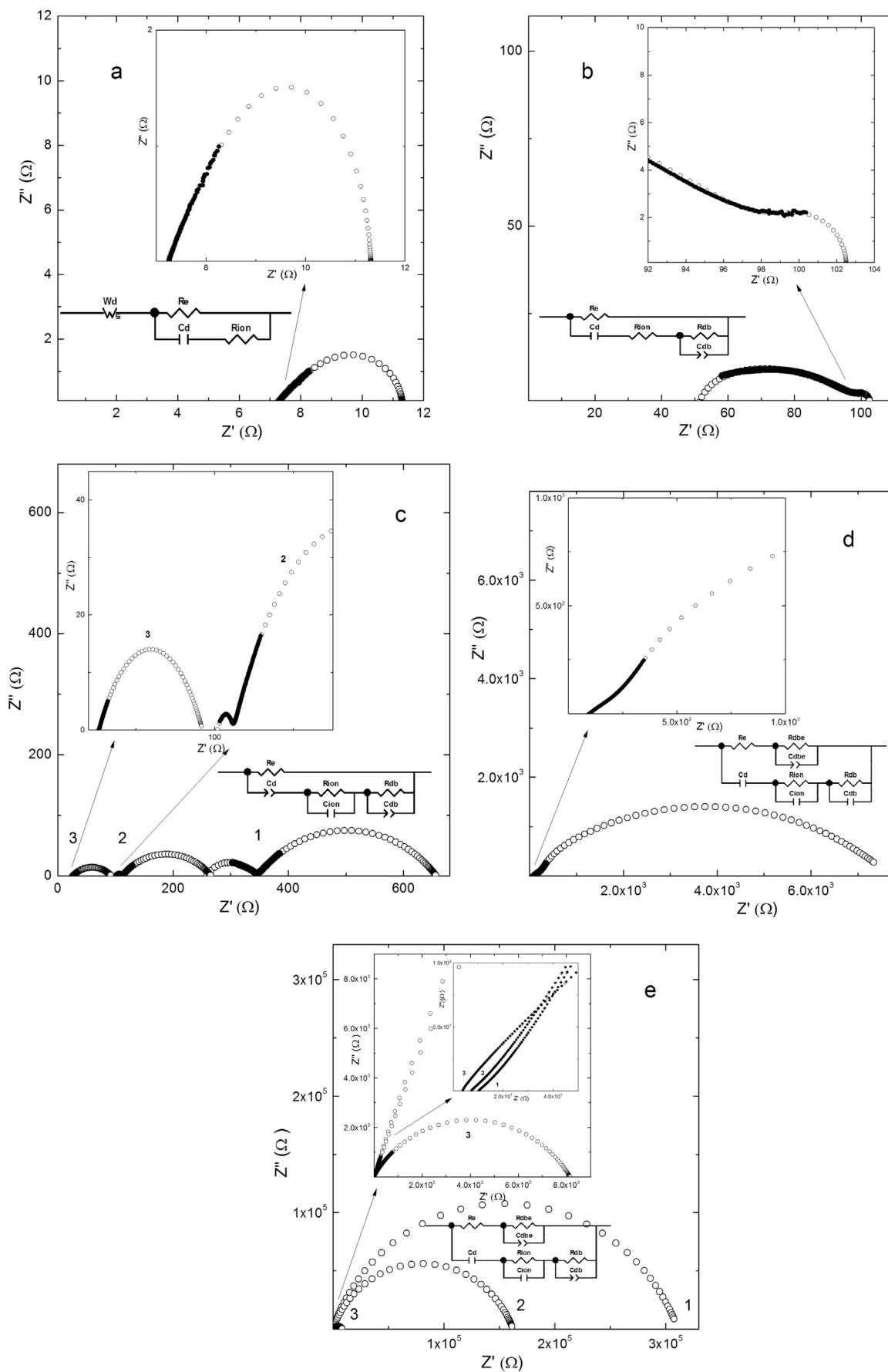
Fig. 2. Nyquist plots at $T = 298$ K for Cu_7SiS_5I (a), $(Cu_{0.75}Ag_{0.25})_7SiS_5I$ (b), $(Cu_{0.5}Ag_{0.5})_7SiS_5I$ (c), $(Cu_{0.25}Ag_{0.75})_7SiS_5I$ (d), and Ag_7SiS_5I (e): experimental data (solid dots), calculated data (open dots) and EEC. For $(Cu_{0.5}Ag_{0.5})_7SiS_5I$ (c) and Ag_7SiS_5I (e) Nyquist plots are presented at various temperatures: 298 K (1c), 303 K (1e), 323 K (2), 373 K (3).

to the bulk ion elements in EEC, the electron resistance of R_e is included, and in the case of $(Cu_{0.25}Ag_{0.75})_7SiS_5I$ mixed crystal, the electronic resistance consists of the sum of the bulk electronic resistance R_e and the electronic resistance of the domain boundaries R_{dbe} which are characterized by the capacity C_{dbe} (Fig. 2d). This tendency is observed due to the growth of ionic component of conductivity ($\sigma_{ion} > \sigma_{el}$).

The analysis of the temperature behavior of the Nyquist plots in mixed crystals is given by the example of $(Cu_{0.5}Ag_{0.5})_7SiS_5I$ (Fig. 2c). With increasing temperature, the growth of electronic conductivity gradually reduces the influence of diffusion ionic processes in the bulk of the crystal, as evidenced by the decrease of the high-frequency semicircle at 323 K (Fig. 2c, curve 2). With further increase of temperature up to 373 K (Fig. 2c, curve 3) there is a further reduction of the influence of diffusion ionic processes in the bulk of the sample, which, together with the decrease in the thickness of the double diffusion layer, eventually leads to the complete disappearance of the high-frequency semicircle.

It should be noted that the ionic conductivity of $(Cu_{1-x}Ag_x)_7SiS_5I$ mixed crystals with x = 0.25, 0.5, 0.75 is determined by the sum of the ionic resistance of the sample R_{ion} and the resistance of the domain boundaries R_{db}, whereas the ionic conductivity is limited by the presence of the above mentioned domain boundaries (Fig. 2b, c, d).

Ag_7SiS_5I crystal is characterized by a very low electron conductivity ($\sigma_{ion} \gg \sigma_{el}$), which caused even greater shift of the low-frequency semicircle into the low-frequency area, which is the evidence of an increase in the influence of diffusion and relaxation processes. Unfortunately, due to the low frequency limitation (20 Hz) of measurements, we were not able to determine the electronic conductivity of Ag_7SiS_5I at temperatures of 292 K and 298 K with sufficient accuracy. Therefore, Fig. 2e shows the Nyquist plot at 303 K. The low-frequency semicircle, as in the previous case, is described by the parameters responsible for ion resistance, the capacity of the domain boundaries, and the capacity of the double diffusion layer. The predominant influence of diffusion and relaxation ionic processes, against which the low specific values of electron and ionic conductivity, lead to the fuzzy representation of the high-frequency semicircle, due to the reduction of the influence of the bulk conductivity of the sample (Fig. 2e). The description of the processes corresponding to the EEC (Fig. 2e) is similar to the case described for $(Cu_{0.25}Ag_{0.75})_7SiS_5I$ mixed crystal. EEC displayed in the Fig. 2e shows the temperature behavior of the Nyquist plots for Ag_7SiS_5I crystal in the studied temperature range, which is in good agreement with the description of ionic and electronic processes according to the EEC. This is evidenced by the degeneration of two semicircles into one at 373 K due to further reducing the influence of bulk parameters (R_{ion}, C_{ion}) for Ag_7SiS_5I crystal.

The nature of the domains for individual Cu_7SiS_5I and Ag_7SiS_5I crystals as well as for $(Cu_{1-x}Ag_x)_7SiS_5I$ mixed crystals with x = 0.25, 0.5, 0.75, may be associated with the presence of mosaic crystal texture. In this case, the domain boundaries represent a structural non-homogenity, which manifests itself in the disorientation of the texture elements < 1° [19].

The analysis of impedance spectra by means of ECC for $(Cu_{1-x}Ag_x)_7SiS_5I$ mixed crystals allowed to study the compositional behavior of the ionic and electronic components of electrical conductivity, which is shown in Fig. 3a. It was established that the compositional dependence of the ionic conductivity is nonmonotonic and nonlinear. The ionic conductivity of Cu_7SiS_5I at 298 K is 0.003 S/cm, while Ag_7SiS_5I is characterized by a slightly higher ionic conductivity of 0.008 S/cm, which is associated with greater disordering of the Ag moving positions compared to the positions of Cu in the crystal lattice.

Let us consider the mechanism of ion transport in $(Cu_{1-x}Ag_x)_7SiS_5I$ mixed crystals. For Cu_7SiS_5I crystal, although the positions Cu1 (24 g) are in the plane of the triangle S1S2S1, the mobile in the structure is an atom at the position Cu2 (48 h), which is shifted to the plane S1I1S2 and to the edge S2I (Fig. 4a). This is explained by the lower value of site occupation factor (SOF) of Cu2 (0.301) as compared to Cu1 (0.561).
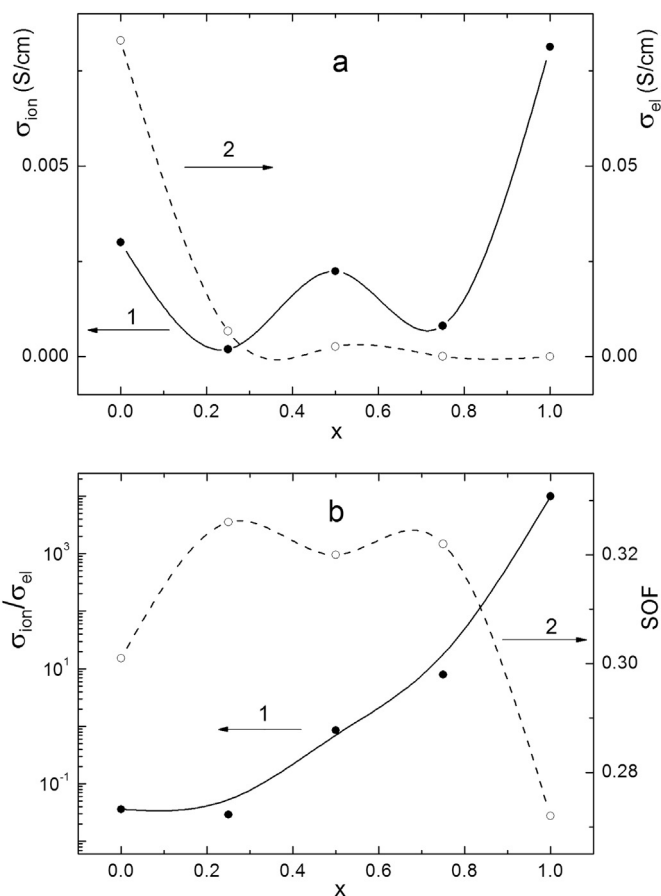

Fig. 3. Compositional dependences of the ionic and electronic components of the electrical conductivity (a), SOF of the mobile positions in the "conductivity net" and the ratio of ionic to electronic conductivity (b) for $(Cu_{1-x}Ag_x)_7SiS_5I$ mixed crystals at $T = 298$ K.

While formation of a mixed crystal, the determining factor in conductivity is the position of substitution of Cu2Ag2 due to the shift to the triangles (S1I1S2) and the S2I1 edges. For Ag_7SiS_5I crystal, similarly to Cu_7SiS_5I, the position of Ag2 (48 h) is most mobile (Fig. 4b).

So, the site occupancy factor for the position of the silver atoms is SOF (Ag2) = 0.272, while for the copper atoms - SOF (Cu2) = 0.301. The observed two conductivity minima for $(Cu_{0.75}Ag_{0.25})_7SiS_5I$ and $(Cu_{0.25}Ag_{0.75})_7SiS_5I$ and one small conductivity maximum for $(Cu_{0.5}Ag_{0.5})_7SiS_5$ also agree well with the SOF values of mobile positions Cu (Ag) in crystal lattices (Fig. 3a and b). At the same time, the value of the electronic conductivity, which for Cu_7SiS_5I is 0.083 S/cm, during the Cu → Ag substitution decreases and for Ag_7SiS_5I, it is ~8.23 × 10^{-7} S/cm (Fig. 3a).

Since one of the main characteristics of superionic materials is the ratio of ionic to electronic conductivity, then in Fig. 3b its compositional dependence is given. It was established that at the transition from Cu_7SiS_5I crystal, for which the electronic conductivity is 28 times higher than the ionic one, to the Ag_7SiS_5I crystal, the σ_{ion}/σ_{el} ratio tends to increase and for the Ag_7SiS_5I crystal the ionic conductivity is almost five orders of magnitude higher than the electronic one.

Fig. 5 shows the temperature dependences of the ionic and electronic components of conductivity in the Arrhenius coordinates. It is shown that they are linear and are described by the Arrhenius law, which testifies to the thermoactivation mechanism of conductivity. Due to them, the values of activation energy were determined, both for the ionic and for the electronic components of conductivity (Fig. 6). On the compositional dependence of the activation energy of ionic conductivity, a nonlinear increase in the activation energy with maximum
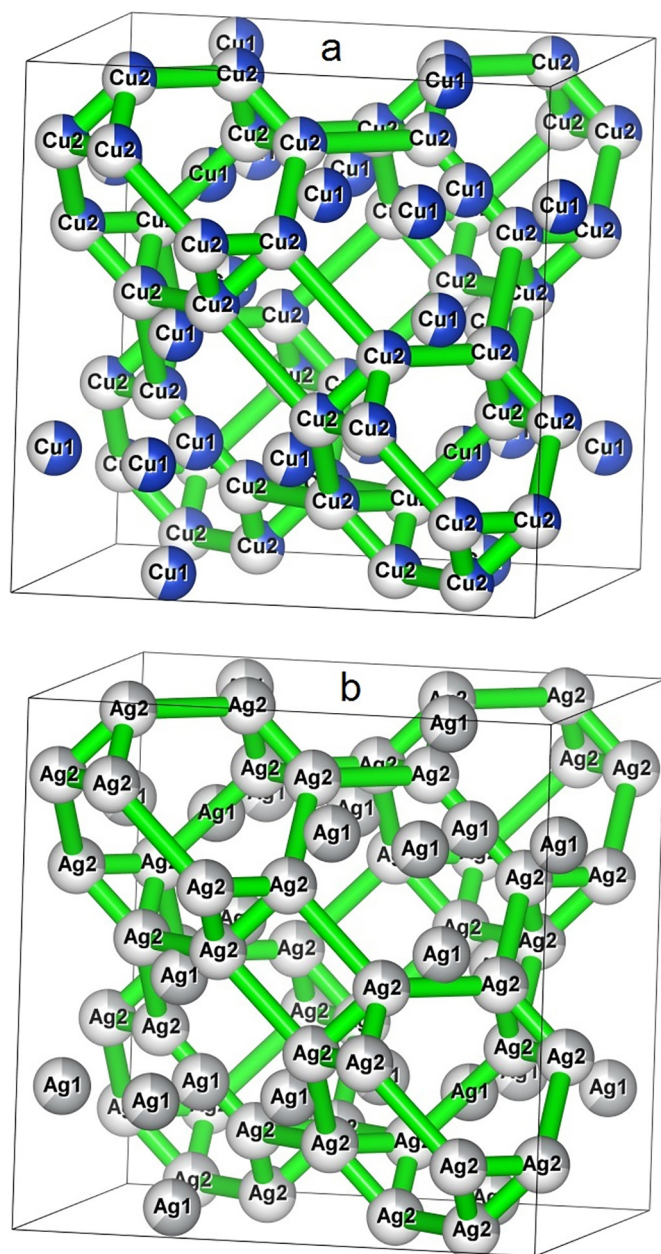
Fig. 4. Illustration of the mechanism of ion transport in Cu_7SiS_5I (a) and Ag_7SiS_5I (b) crystals on the example of mobile cations migration "net".

for $(Cu_{0.5}Ag_{0.5})_7SiS_5I$ (E_a^{ion} = 0.757 eV) is observed. The increase of the activation energy in the mixed crystals in comparison with Cu_7SiS_5I (E_a^{ion} = 0.173 eV) and Ag_7SiS_5I (E_a^{ion} = 0.435 eV) is associated with the increasing influence of compositional disordering that prevents the process of ion transport. At the same time, the activation energy of the electronic conductivity also increases nonlinearly at the transition from Cu_7SiS_5I (E_a^{el} = 0.247 eV) to Ag_7SiS_5I (E_a^{el} = 1.04 eV), although without visible peculiarities (Fig. 6).

4. Conclusions

Synthesis and growth of $(Cu_{1-x}Ag_x)_7SiS_5I$ mixed crystals were performed. Alloys in Cu_7SiS_5I – Ag_7SiS_5I system were synthesized by a direct one-temperature method from pre-synthesized Cu_7SiS_5I та Ag_7SiS_5I. $(Cu_{1-x}Ag_x)_7SiS_5I$ mixed crystals were grown by crystallization from a melt.

Investigation of electrical conductivity for $(Cu_{1-x}Ag_x)_7SiS_5I$ mixed

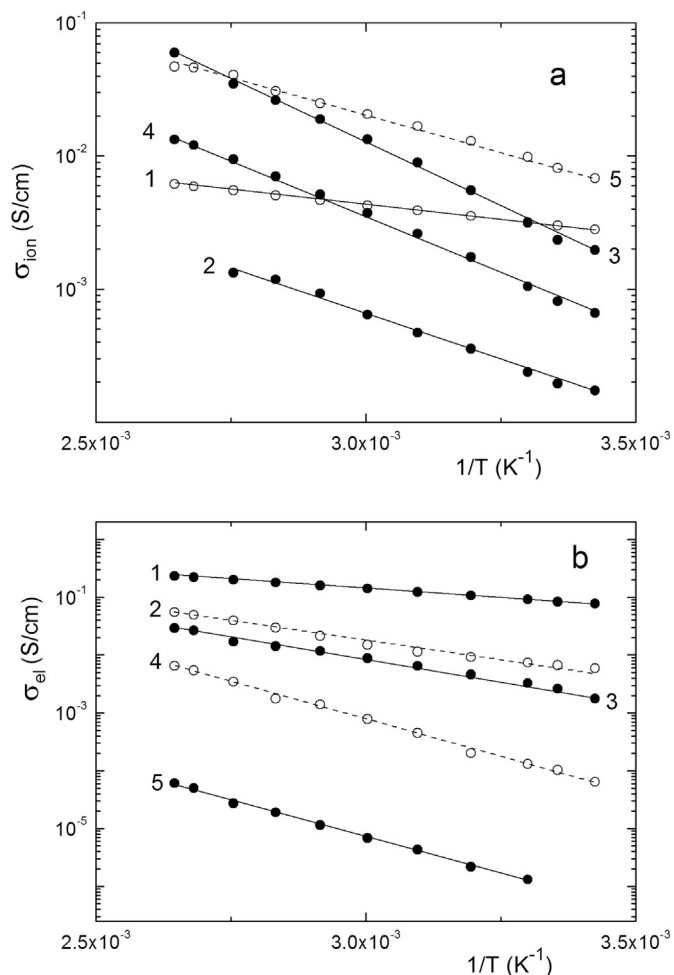Fig. 5. The temperature dependences of the ionic (a) and electronic (b) components of electrical conductivity for $(Cu_{1-x}Ag_x)_7SiS_5I$ mixed crystals: Cu_7SiS_5I (1), $(Cu_{0.75}Ag_{0.25})_7SiS_5I$ (2), $(Cu_{0.5}Ag_{0.5})_7SiS_5I$ (3), $(Cu_{0.25}Ag_{0.75})_7SiS_5I$ (4), Ag_7SiS_5I (5).

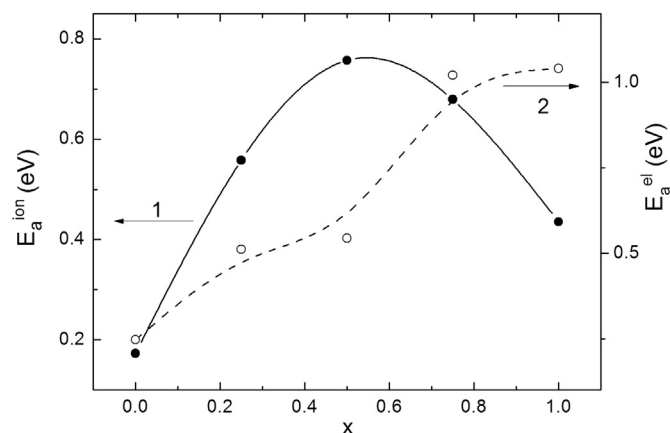Fig. 6. Compositional dependences of the activation energy of the ionic (1) and electronic (2) components of electrical conductivity for $(Cu_{1-x}Ag_x)_7SiS_5I$ mixed crystals.

crystals was carried out by the method of impedance spectroscopy in the frequency range from 20 Hz to 2×10^6 Hz and in the temperature range 292–378 K. Measurements were performed by a two-electrode method on blocking gold contacts. The frequency dependences of the total electrical conductivity showed a growth of conductivity with

increasing frequency for all mixed crystals. Nyquist plots were presented and their detailed analysis was carried out using electrode equivalent circuits, which allowed to separate the contributions of the ionic and electronic components to the total electrical conductivity.

It was revealed that the compositional dependence of the ionic conductivity is nonmonotonic and nonlinear with two minima for $(Cu_{0.75}Ag_{0.25})_7SiS_5I$ and $(Cu_{0.25}Ag_{0.75})_7SiS_5I$, and it increases with the transition from Cu_7SiS_5I (0.003 S/cm) to Ag_7SiS_5I (0.008 S/cm). The peculiarities of the compositional dependence of the ionic conductivity also agree well with the SOF values of the mobile positions of Cu (Ag) in crystal lattices. Electronic conductivity with an increase of silver content nonlinearly decreases with a downhill by more than five orders of magnitude for Ag_7SiS_5I compared to Cu_7SiS_5I. The analysis of the compositional dependence of the ratio of ionic conductivity to the electronic one showed that due to $Cu^+ \rightarrow Ag^+$ cationic substitution it is nonlinearly increasing by almost five orders of magnitude.

The Arrhenius character of the temperature dependences of the ionic and electronic components of conductivity for $(Cu_{1-x}Ag_x)_7SiS_5I$ mixed crystals is established, indicating their thermoactivation mechanism. At $Cu^+ \rightarrow Ag^+$ cationic substitution a nonlinear increase in the activation energy of both ionic conductivity and electronic conductivity was observed, and in the first case with a maximum for $(Cu_{0.5}Ag_{0.5})_7SiS_5I$ mixed crystal.

References

[1] W.F. Kuhs, R. Nitsche, K. Scheunemann, The argyrodites – a new family of the tetrahedrally close-packed structures, Mater. Res. Bull. 14 (1979) 241–248.

[2] T. Nilges, A. Pfitzner, A structural differentiation of quaternary copper argyrodites: structure – property relations of high temperature ion conductors, Z. Kristallogr. 220 (2005) 281–294.

[3] M. Laqibi, B. Cros, S. Peytavin, M. Ribes, New silver superionic conductors Ag_7XY_5Z (X = Si, Ge, Sn; Y = S, Se; Z = Cl, Br, I) – synthesis and electrical studies, Solid State Ionics 23 (1987) 21–26.

[4] A. Dziaugys, J. Banys, A. Kežionis, V. Samulionis, I. Studenyak, Conductivity investigations of Cu_7GeS_5I family fast-ion conductors, Solid State Ionics 179 (2008) 168–171.

[5] I.P. Studenyak, M. Kranjčec, M.V. Kurik, Urbach rule and disordering processes in $Cu_6P(S_{1-x}Se_x)_5Br_{1-y}I_y$ superionic conductors, J. Phys. Chem. Solids 67 (2006) 807–817.

[6] A.F. Orliukas, E. Kazakevicius, A. Kezionis, T. Salkus, I.P. Studenyak, R.Yu. Buchuk, I.P. Prits, V.V. Panko, Preparation, electric conductivity and dielectrical properties of Cu_6PS_5I-based superionic composites, Solid State Ionics 180 (2009) 183–186.

[7] I.P. Studenyak, M. Kranjčec, V.V. Bilanchuk, O.P. Kokhan, A.F. Orliukas, E. Kazakevicius, A. Kezionis, T. Salkus, Temperature variation of electrical conductivity and absorption edge in Cu_7GeSe_5I advanced superionic conductor, J. Phys. Chem. Solids 70 (2009) 1478–1481.

[8] T. Šalkus, E. Kazakevičius, J. Banys, M. Kranjčec, A.A. Chomolyak, Yu.Yu. Neimet, I.P. Studenyak, Influence of grain size effect on electrical properties of Cu_6PS_5I superionic ceramics, Solid State Ionics 262 (2014) 597–600.

[9] I.P. Studenyak, M. Kranjčec, V.Yu. Izai, A.A. Chomolyak, M. Vorohta, V. Matolin, C. Cserhati, S. Kökényesi, Structural and temperature-related disordering studies of Cu_6PS_5I amorphous thin films, Thin Solid Films 520 (2012) 1729–1733.

[10] H.-J. Deiseroth, S.-T. Kong, H. Eckert, J. Vannahme, C. Reiner, T. Zaiß, M. Schlosser, Li_6PS_5X: a class of crystalline Li-rich solids with an unusually high Li + mobility, Angew. Chem. Int. Ed. 47 (2008) 755–758.

[11] S. Boulineau, M. Courty, J.-M. Tarascon, V. Viallet, Mechanochemical synthesis of Li-argyrodite Li_6PS_5X (X = Cl, Br, I) as sulfur-based solid electrolytes for all solid state batteries application, Solid State Ionics 221 (2012) 1–5.

[12] C. Yu, L. van Eijck, S. Ganapathy, M. Wagemaker, Synthesis, structure and electrochemical performance of the argyrodite Li_6PS_5Cl solid electrolyte for li-ion solid state batteries, Electrochim. Acta 215 (2016) 93–99.

[13] S. Wenzel, S.J. Seldmaier, C. Dietrich, W.G. Zeier, J. Janek, Interfacial reactivity and interphase growth of argyrodite solid electrolytes at lithium metal electrodes, Solid State Ionics 318 (2018) 102–112.

[14] I.P. Studenyak, O.P. Kokhan, M. Kranjčec, M.I. Hrechyn, V.V. Panko, Crystal growth and phase interaction studies in Cu_7GeS_5I–Cu_7SiS_5I superionic system, J. Cryst. Growth 306 (2007) 326–329.

[15] A.V. Bendak, O.O. Yamkoviy, V.V. Bilanchuk, I.P. Studenyak, Peculiarities of compositional disordering in crystals of $Cu_7(Ge_{1-x}Si_x)S_5I$ solid solution, Scientific Herald of Uzhgorod Univversity: Ser. Physics 36 (2014) 37–40. (in Ukrainian).

[16] M.E. Orazem, B. Tribollet, Electrochemical Impedance Spectroscopy, John Wiley & Sons, New Jersey, 2008.

[17] A.K. Ivanov-Schitz, I.V. Murin, Solid State Ionics, vol. 1, S.-Petersburg Univ. Press, 2000 (in Russian).

[18] R.A. Huggins, Simple method to determine electronic and ionic components of the conductivity in mixed conductors: a review, Ionics 8 (2002) 300–313.

[19] R.A. West, Solid State Chemistry and its Applications, John Wiley & Sons, New Jersey, 2014.